JOURNAL OF MATERIALS SCIENCE 28 (1993) 1738–1748

Dual-beam CO_2 laser cutting of thick metallic materials

P. A. MOLIAN
Mechanical Engineering Department, Iowa State University, Ames, IA 50011, USA

A dual-beam technique involving two CO_2 gas lasers with a power capacity of 1.5 kW each, was used to cut steel and superalloy. A comparison with single-beam CO_2 laser cutting showed that dual beams were capable of enhancing the cutting thickness and speed without deteriorating the quality of cut. Heat-conduction models, assuming the laser beams as line sources, were used to estimate the cutting thickness and speed as a function of distance between the two laser beams. Experimental data, coupled with theoretical modelling, have provided a new concept, namely stretching the width of the laser beam in the direction of cutting to cut thicker section solids at moderate speeds.

1. Introduction

The first practical applications of high-power lasers were machining and welding, with machining currently constituting the largest single application (over 50%) of lasers in manufacturing. Laser cutting is a thermal process that results in higher quality and precision than other thermal processes. The laser is capable of delivering a high concentration of energy ($> 10^9$ J cm^{-2}) to a very small area (> 1 to several hundred micrometres diameter) making it possible to melt and evaporate almost all materials. Both high-power CO_2 and Nd:YAG lasers are being used for cutting in aerospace, automotive, electronics, and defense industries. For example, it has been reported [1] that an unassisted Nd:YAG laser was capable of cutting 0.635 mm (0.025 in) thick Hastelloy-X (a superalloy) sheet at a rate of 5 mm s^{-1} (12 in min^{-1}) as compared with the 0.42 mm s^{-1} (1 in min^{-1}) cutting rate of a computer numerically controlled (CNC) three-axis milling machine. In addition to the advantages of high speed, tight tolerances, and good cut-surface quality, the laser is ideal for interfacing with robots in computer-aided design/computer-aided manufacturing (CAD/CAM) systems, allowing the efficient and cost-effective manufacture of parts for specific applications. In fact, with proper software design, each laser-manufactured part could be different with little or no increase in machine time.

Other applications of lasers in machining depend on the laser's ability to produce structures and cut materials not possible with conventional machining methods, relying on such laser attributes as narrow heat-affected zone, narrow kerf, shallow angle hole, large aspect ratio holes, very small diameter holes, odd shapes, cavities and slots, machining of inaccessible locations, noncontact machining (no tool force), machining of soft as well as very hard materials, and cutting very brittle and very ductile materials. The competitive machining methods such as electrochemical machining, electrical discharge machining, and chemical machining (which have been developed to overcome some of the problems encountered with conventional tool machining) suffer from drawbacks such as low speed, low production yield, poor surface integrity, difficulty in making deep and narrow cuts, and marginal tolerances.

Commonly, a laser can be used in three different ways to cut a variety of materials [2]: sublimation cutting, fusion cutting, and gas cutting. In laser sublimation cutting, a focused laser beam evaporates the material, and a jet of inert gas, coaxial to the beam, carries away the vapour. Although narrow kerf width with a high-quality surface can be generated by this technique, it is limited to only thin sections. In laser fusion cutting, the laser beam heats a material to above its melting point and the use of a high-pressure, inert gas blows the molten material out of the kerf. A noteworthy advantage of this method is the increased cutting rate, but drawbacks include striations on the cut surface and solidified droplets of residual melt clinging at the lower cut edge. In laser gas cutting, a reactive gas such as oxygen is used coaxially with the laser beam. Chemical energy released from the exothermic reaction aids in cutting; thus, high cutting rates are obtained. Other methods of laser cutting involve burning in a reactive gas, thermal stress fracture, and scribing.

The current thrust in laser cutting lies in extending its limitations in terms of cutting speed, thickness and quality. This will allow tighter tolerances and reduction in production costs. New laser-machining procedures are sought for cutting thicker iron and steel (> 10 mm), and to increase the speed at which lasers machine superalloys, ceramics and composites. It is well known that a limitation is machining thicker materials (in general > 6 mm for metals; see also Fig. 1) with lasers. Most applications of laser cutting utilize an oxygen or air–gas assist. The reaction of

0022–2461

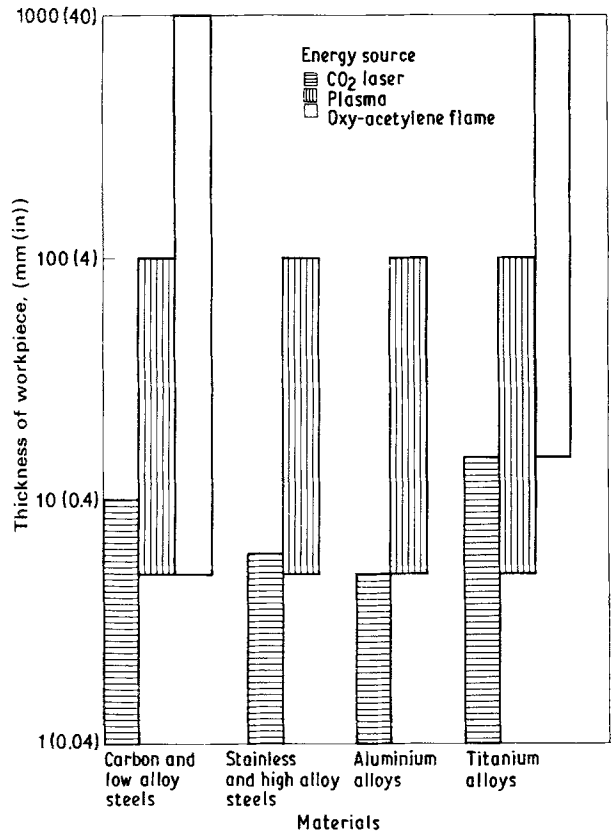

Figure 1 A comparison of thermal cutting systems with the thickness of workpiece.

oxygen with the metal to form an oxide produces additional heat that aids in melting the material, and the gas jet cleans the cut by blowing the molten droplets from the cut region, cools the unmelted adjoining regions by convection, reduces the heat-affected zone (HAZ), and protects the focusing lens from droplets and reaction products.

A literature review of the various aspects of laser cutting of solids reveals that the following should be considered for cutting thicker-section solids.

1. Higher power lasers with a TEM_{00} mode beam quality [3].
2. Lower Fresnel number or smaller beam size.
3. Optimal focusing. For example, the focus should be at one-third of the cutting thickness [4].
4. Optimal reactive gas-flow conditions using a modified nozzle design [5]. For instance, a three-way nozzle generated supersonic gas flow and permitted cutting of thicker steel plates [5].
5. Additional heat sources such as an electric arc [6], or using organic gases such as acetylene [7].
6. Absorption of laser power by improving the energy coupling.
7. Prevention of plasma formation.
8. Selection of a material with favourable thermal and chemical properties.
9. Optimal cutting speed, because otherwise self-burning or incomplete penetration of heat may occur.
10. Excellent fluidity of slag or molten metal for easier removal.

Cutting thin sheets involves high temperatures and results in a quasisublimation process. When thick plates are cut, the temperature at the cutting front will be less and the amount of vaporized material is negligible. A considerable amount of slag forms during cutting, in which case the reaction rate is controlled by the diffusion rate of oxygen. Thicker-section laser cutting may be considered to be a reactive gas fusion cutting in which the laser beam creates a "key hole" into the workpiece. The hole is surrounded by oxidized molten metal which closes the hole when the beam travels in the cutting direction. The melting isotherm penetrates into the workpiece as the pressure from the oxygen gas blows away the molten metal and slag.

An understanding of heat and fluid flow, combustion reaction phenomena, and gas-flow dynamics is essential to develop a satisfactory theoretical model for predicting thicker-section cutting. From the experimental point of view, additional energy, in the form of a heat source, should be deposited for preventing the "blind" cut in thicker sections. Hence, a thorough understanding of the physical nature of the problem through analytical and experimental treatment is a prerequisite to the development of any innovative technology for laser cutting of thick solids, the basic objective of the paper.

2. Modelling of laser cutting

Laser cutting requires careful control of several parameters including beam mode quality, beam diameter, focusing, distance between the nozzle and workpiece and assist-gas pressure. It will be very useful, as a result, to be able to predict experimental trends theoretically to achieve a better understanding of the physics of the process. Laser cutting models available in the literature are essentially based on the classical conduction heat transfer equations and are analytically or numerically solved by making the following assumptions.

1. Thermal properties of the material are independent of temperature.
2. A laser beam is considered to be a moving-point source of heat.

Usually, the classical conduction theory can be applied to the laser heating process because of the fact that the heating time is much longer than the time between collisions for the free electrons within the workpiece [2]. The governing differential equation is

$$V/\alpha + \Delta^2 T(x, y, z, \theta) - 1/\alpha \partial T/\partial t(x, y, z, \theta) = -Q(x, y, z, \theta)/K \quad (1)$$

where T is the temperature (K), α the thermal diffusivity ($m^2 s^{-1}$), K the thermal conductivity ($W m^{-1} K^{-1}$), V the velocity of the workpiece ($m s^{-1}$), Q the heat source, heat per unit volume per unit time ($J m^{-3} s^{-1}$) and θ the time (s). The equation has been solved for several problems concerning thin sheet metal cutting. In all analytical treatments, the nonlinear term due to radiation is neglected, and so is convection loss. Furthermore, for thin sheets, the temperature is assumed to be independent of depth, transforming the problem into a two-dimensional one.

Decker *et al.* [8] presented a simple thermal model to estimate the maximum cutting speed, according to which

$$V = \frac{P_L}{ets(\Delta G_S - \Delta G_R)} \quad (2)$$

where V is the cutting speed (m s^{-1}), P_L the absorbed laser power (W), e the density (kg m^{-3}), t the thickness of the workpiece (m), s the kerf width (m), ΔG_S the sublimation energy per unit mass (J kg^{-1}), and ΔG_R the heat of reaction per unit mass (J kg^{-1}). This model assumes laser sublimation cutting in which the material vaporizes and chemically reacts with the oxygen gas. Neglected effects include heat loss due to the heat transfer into the workpiece, thermal radiation, and cooling by the assist gas. The cutting speed predicted by this model underestimated the experimental value and was explained [8] to be due to two reasons.

1. The kerf width is not equal to the beam diameter, as assumed in the model.
2. All the cut material is not vaporized.

However, this model provides a rough estimate of cutting speed, restricted to cutting of thin sections.

Kamalu and Steen [2] presented Equation 2 in a different form by considering that the laser energy is used in melting and evaporating the material and none is lost by conduction, convection, and radiation

$$V = \frac{P_L}{ets(C_p \Delta T + L_f + m' L_v)} \quad (3)$$

where ΔT is the temperature rise to the melting point (K), C_p the specific heat (J kg^{-1} K^{-1}), L_f the latent heat of fusion (J kg^{-1}), m' the mass fraction evaporated, and L_v the latent heat of evaporation (J kg^{-1}).

The temperature distribution in the material during cutting can be found by solving the conduction Equation 1. Ready [9] gives the one-dimensional solution for the temperature distribution as

$$T(Z, \theta) = \left[\frac{2P_L(\alpha\theta)^{1/2}}{K}\right] \text{ierfc}\left[\frac{Z}{2(\alpha\theta)^{1/2}}\right] \quad (4)$$

where θ is the interaction time (s), and Z the depth (m).

The solution of heat conduction Equation 1, assuming the laser beam to be a point source located at (x^1, y^1, z^1), is given [10] by

$$T(x, y, z, \theta) = \frac{Q(x^1, y^1, z^1)}{8(\pi\alpha\theta)^{3/2}} \times \exp - \frac{(x - x^1)^2 + (y - y^1)^2 + (z - z^1)^2}{4\alpha\theta} \quad (5)$$

For thin sheet metal cutting, Equation 5 is reduced to

$$T(r, \theta) = \frac{Q}{4\pi kt\theta} \exp\left(\frac{-r^2}{4\alpha\theta}\right) \quad (6)$$

where $r = (x^2 + y^2)^{1/2}$ and $t^2/4\alpha\theta \ll 1$.

Assuming the laser beam to be a moving-point source of heat, Duley and Gonsalves [11] have shown that for thin-section metal cutting

$$\exp\left(\frac{Vx}{2\alpha}\right) = \frac{2\pi ktT}{(fP_L + P_1 - P_2)K_0(rV/2\alpha)} \quad (7)$$

where T is the temperature at the point (x, y) (K), K_0 the Bessel function of second kind and zeroth order, $r = (x^2 + y^2)^{1/2}$, f the fraction of the laser beam actually striking the sheet, P_1 the chemical power, P_2 the power dissipated because of the cooling effect of the jet $= \beta F^1 K_1 (T - T_g)$, (where β = fraction of the incident gas that cools the material and F^1 is the collision rate of oxygen molecules with the material, $= (6.03 \times 10^{23} F/60 \times 2.24 \times 10^4)$ where F = gas flow rate, (m^3 s^{-1}), T the material temperature (K), T_g the gas temperature (K) and K_1 is Boltzmann's constant). Using approximate calculations, Duley and Gonsalves [11] have shown that P_2 is generally small except at large values of F.

Babenko and Tychinskii [12] have developed a heat flow model for cutting of relatively thick plates that takes into account the chemical reaction energy. They started with the power balance equation as $P = P_L + P_1 - P_2$, where P is the total power, and wrote the classical heat conduction equation incorporating the chemical power as

$$W_L = \frac{P_L - P_2}{2\pi KtT_0} = \exp\left(\frac{Vx}{2\alpha}\right) K_0^{-1}\left(\frac{Vr}{2\alpha}\right) - \frac{2}{\pi}\psi\left(\frac{vy}{2\alpha}\right) \quad (8)$$

where T_0 is the temperature at the kerf wall (K), and ψ the thermochemical parameter $= Q_c/(C_p T_0)$ where Q_c is the specific energy yield of chemical reactions.

An approximate numerical solution of Equation 8 is given by

$$W_L = \frac{2}{\pi}\left(\frac{vy}{2\alpha}\right)(1.9 - \psi) + 0.3 \quad (9)$$

Equation 9 shows that if $\psi < 1.9$ then $\partial W_L/\partial v > 0$, which means that an increase of $(vy/2\alpha)$ results in a rise of W_L and corresponds to steady-state cutting conditions. If the quantity W_L is negative, then cutting is accomplished solely at the expense of chemical reaction energy.

Kamalu and Steen [2] compared the results of simple heat balance, moving line source, and moving cylindrical source models with experimental data and concluded that the simple heat balance and line source models exaggerate the cutting speeds. Bunting and Cornfield [13] attempted to establish a more general theory of thermal cutting by assuming the laser beam as a cylindrical heat source. They developed a relationship between the power density and the cutting speed in terms of thermal properties of the material. Bunting and Cornfield [13] claimed that Equation 7 will give inaccurate results if the characteristic length of line source $(2\alpha/v)$ is equal to or less than the cut width, S. These investigators modified Equation 7 and established a relationship as

$$I(w) = \frac{8Kt(T_{mp} - T_0)}{P_1 S^2} \quad (10)$$

where

$$I(w) = \int_0^1 r^1 \, dr^1 \int_0^{2\pi} (e^{-wr^1 \cos\theta}) K_0 \times w(r^{1^2} - 2r^1 \sin\theta + 1)^{1/2} \, d\theta$$

with $w = VS/4\alpha$, and T_{mp} is the melting point (K). Schuöcker and Abel [14] analysed the mechanisms of material removal during laser cutting and developed several equations of heat and gas flow. From movies showing the laser cutting process, erosion takes place at a nearly vertical plane at the momentary end of the cut. That plane is covered by a thin molten layer that is further heated by absorbed laser radiation and by chemical reaction. The removal of material from that layer is carried out by evaporation and by ejection of molten material due to the friction between the melt and the reactive gas flow. This description indicates that the high-temperature molten layer is the actual cutting tool. Schuöcker's model, described above, yielded the energy and mass balance equations from which all information on the details of the cutting process can be obtained.

Rothe and Sepold [4] presented the important requirements for cutting thick plates with oxy-assisted lasers. Assuming the beam as a line source, they developed a model that yielded the following conclusions.

1. The focus should be positioned at one-third of cutting thickness.
2. The kerf width, S, is written as $S = (\alpha_1 d_1 t)^{1/2}$ where α_1 is the focusing angle, d_1 the depth of field, and t the thickness of the plate.
3. The minimal laser power, P_{min}, for oxygen-assisted cutting depends on the material properties and on cutting thickness. For steel, $P_{min} = 80\ t$ where P_{min} is in watts, t in millimetres.
4. The chemical reaction of steel and oxygen is limited by the mass transport coefficient $M = 6\ mm\ s^{-1}$.
5. The maximum cutting speed for a supersonic gas flow velocity of $450\ m\ s^{-1}$ is $V_{max} = 5.3\ m\ s^{-1}\ (S/t)$.

3. Concept of thicker-section metal cutting with dual beams

In laser cutting, two significant problems are the coupling of laser energy into the workpiece and plasma formation at the workpiece surface. Most metals tend to reflect 90% or more of the CO_2 laser energy. When the intensity of the laser beam becomes sufficiently high ($> 10^8\ W\ cm^{-2}$), plasma formation occurs and prevents coupling of the laser energy into the workpiece. A prudent approach is to use two high-power CO_2 laser beams (separated by a small distance) in order to increase the coupling efficiency by minimizing laser/plasma interactions, and taking advantage of the increased absorptance of the melt relative to the solid metal.

Let us now consider the cutting of thick solids by the application of two laser beams (Fig. 2). In this process, the first beam partially penetrates into the moving workpiece, causing regions of the material to be melted and vaporized. A cylindrical 'keyhole" bounded by the melting isotherm is created by the first beam. As the material moves under the beam, the "keyhole" also moves with a cutting speed in the steady-state condition. There is some vaporization due to the formation of the keyhole. The first beam creates a "blind" cut because of inadequate energy

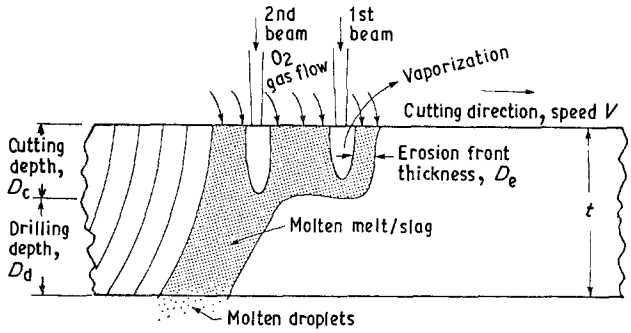

Figure 2 Proposed mechanism of laser cutting with dual beams.

input. As the second laser beam hits the molten region produced by the first beam, it vaporizes some material and superheats the remaining molten material. The combined action of the exothermic reaction of oxygen and the second laser beam aids in drilling through the melt, thereby allowing molten droplets to be ejected. Furthermore, the oxygen gas flow causes some convection currents. The second beam actually cuts through the liquid metal, which means surface reflectivity is not a limitation. As a result, a clean, good quality cut can be expected.

Thermal modelling of dual-beam laser cutting requires considerations of a moving heat source conduction equation and thermodynamics of oxygen–metal chemical reactions. Such equations may be used to estimate the size of "blind cut", D_C, thickness of erosion front, D_e, and temperature of the cutting front.

4. Experimental procedure

4.1. Materials

The materials used in this work were a plain carbon steel (AISI 1018) and a superalloy (Hastelloy C). Carbon steel was chosen because it was extensively used in industries for laser cutting but was limited to a thickness of 8 mm. Superalloys are difficult to machine and cause rapid tool wear in conventional tool machining. The properties of superalloy that contribute to the machining difficulties include: high shear strength that results in high cutting forces at the cutting edges of tools; high capacity for work hardening; the presence of hard, abrasive intermetallic compounds in the microstructures; and low thermal conductivity resulting in heat concentration at the cutting zone and thereby damaging the tool. Conventional tool-machining processes require greater cutting forces and considerable improvement in tool design for machining superalloys.

In laser machining, superalloys do not react with oxygen gas as efficiently as does carbon steel; hence laser-cutting speeds for superalloys are lower than those for comparable thicknesses of carbon and low-alloy steels. Further, the presence of nickel or cobalt raises the viscosity of the molten metal, thus causing it to migrate and adhere to the rear side of the cut. The thermal properties of the alloys used in this work are given in Table I.

TABLE I Thermal properties of the alloys used

Material	Specific heat ($J\,kg^{-1}\,K^{-1}$)	Conductivity ($W\,m^{-1}\,K^{-1}$)	Density ($kg\,m^{-3}$)	Diffusivity ($10^{-6}\,m^2\,s^{-1}$)	Melting temp. (K)
Carbon steel	550	50	7877	11.55	1750
Hastelloy	450	15	8940	3.73	1577

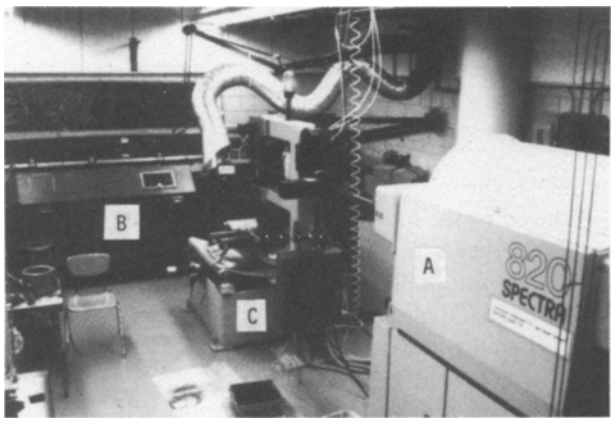

Figure 3 A photograph showing the two laser systems. A, Spectra-physics laser; B, Control laser; C, Five-axis workstation.

4.2. Equipment

Two continuous-wave (CW) CO_2 gas lasers with a power capacity of 1500 W each were used in this investigation. The lasers were manufactured by Spectra-Physics (Model 820) and Control Laser (Model IL 1500). The lasers shared a large workstation that is capable of moving in five axes (three linear, one rotary, one tilting). Fig. 3 shows the lasers and the workstation. The functions of laser and worktable were controlled by a computer numerical controller. The laser beams were circularly polarized to facilitate good quality cutting.

As mentioned previously, one of the important requirements for thicker-section cutting with lasers is the beam's transverse electromagnetic mode (TEM) quality. TEM mode describes the cross-section of a laser-beam profile and is comparable to the sharpness of a cutting tool. TEM_{00} is the lowest order mode that gives rise to a Gaussian energy distribution and is ideal for cutting because it can be focused down to the smallest spot size, thereby giving the maximum energy density. Furthermore, the energy profile across the beam is the same in all axes, an important requirement in profile cutting. For equivalent laser power, the power density of a TEM_{00} mode can be two orders of magnitude greater than the multimode beams that have wide energy distributions.

Both lasers used in this work produced beams with a near TEM_{00} mode, although perfect TEM_{00} is seldom realized in high-power lasers. The rationale for choosing the power levels specified above for this study is its wider usage in metal cutting industries. Higher power lasers than 1.5 kW generally tend to produce a multimode beam configuration (equivalent to a "blunt" cutting tool) with a low degree of output beam stability, generate plasma, and exhibit poor energy-coupling efficiency. Furthermore, higher power lasers cause large thermal problems with optical components in the resonator and in the beam path.

4.3. Dual-beam technique

This method consists in using two CO_2 laser beams along with a supply of oxygen. Fig. 4 shows a schematic illustration of the experimental setup. The two laser beams were brought to the worktable by means of mirrors and a 127 mm focusing lens. The power of each beam was 1500 ± 30 W. The distance between the two beams on the metal plate was 6 mm. The beam was focused at one-third the distance below the workpiece surface. The focused beam size was 0.1 mm. The focused beams were sent through a large nozzle of diameter 10 mm. A reactive oxygen gas was introduced coaxially with the laser beams. The gas pressure was 137 kPa g (20 p.s.i. g) at the nozzle exit. The cutting speed was varied from 4.2–40 mm s^{-1}. The distance between the nozzle and workplate was about 1 mm or less, to concentrate the oxygen gas in the cut zone.

5. Results and discussion

Fig. 5 presents the experimental data obtained using

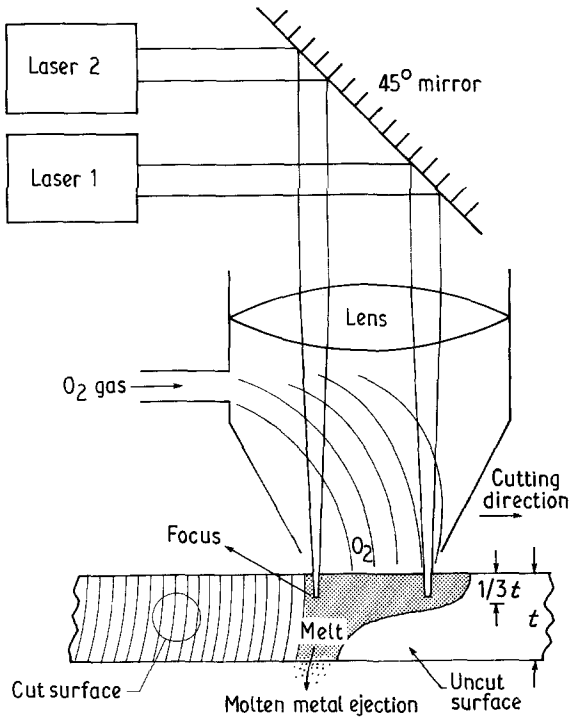

Figure 4 Experimental method for cutting thick solids using two laser beams.

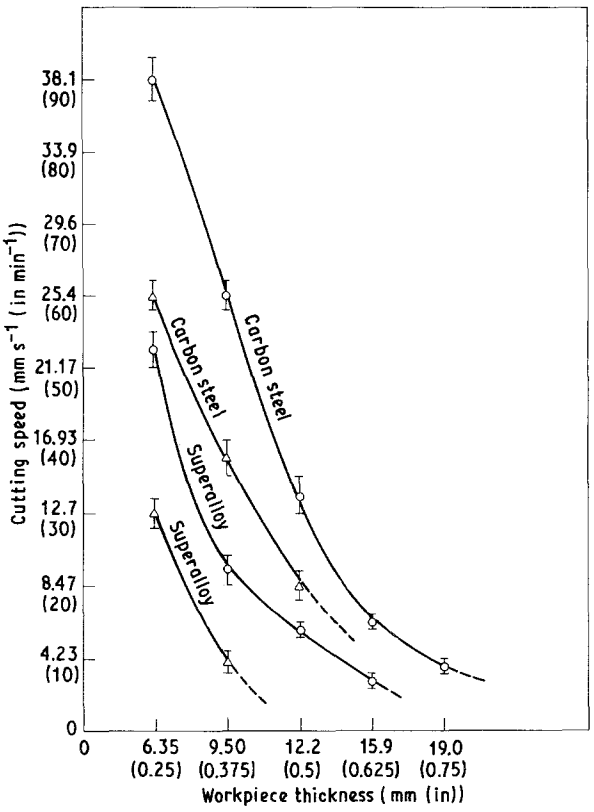

Figure 5 Effects of dual CO_2 laser beams on cutting and thickness. 1.5 kW, CW CO_2 lasers, 127 mm focal length lens. Oxygen assist gas at 413 kPa g (60 p.s.i. g). (○) Dual beam, (△) single beam.

single and dual CO_2 lasers. The significant results are as follows.

1. Dual beams were able to cut thick-sectioned steel and superalloy.
2. For a given section thickness, dual beams increased the cutting speed over the single beam.
3. Carbon steel can always be cut at higher speeds than superalloy. This may be attributed to the oxidation of carbon steel which contributes to increased heat input. Because oxygen can pass freely through the iron oxide layers, and the iron oxide has low viscosity and low adhesion, the force of the oxygen gas jet can readily eject the slag and molten metal. In the case of superalloy which contains chromium and nickel, the oxide layer does not allow oxygen to penetrate through resulting in loss of energy from oxidation and thereby reducing the cutting speed. Furthermore, the viscosity of the superalloy melt is high and hence it is difficult to eject the fluid.

The cut quality, in terms of kerf width, heat-affected zone, surface roughness and taper, deteriorated with an increase in section thickness. However, the kerf at the top surface was narrow and in the range 0.4–1.1 mm. Typical values of kerf width at the top surface are given in Table II. Kerf widths at the top surface are slightly larger for superalloy than for steel. But the kerf widths at the bottom surface are much larger for superalloy than steel. Surface roughness (RMS value) near the top surface was about 5 μm (200 $\times 10^{-6}$ in) and much higher near the bottom surface.

The combined action of two focused laser beams, separated by a distance greater than the keyhole

TABLE II Average kerf width data (top surface)

Thickness (mm)	Kerf (mm)	
	Steel	Superalloy
6.35	0.38	0.46
9.50	0.51	0.65
12.70	0.71	0.83
15.90	0.81	0.94
19.00	1.10	–

width, may be modelled by considering the workpiece preheating above the melting point, T_m, by the first beam and actual cutting by the second beam. According to this model, workpiece preheating improves the deep penetration effect, mainly due to an improvement in the absorption efficiency of the keyhole and a modification of the conduction characteristics inside the workpiece. Because of the fast decrease in steady-state temperature levels when moving off the beam impact region (which is specific to high-power focused beam processing), preheating can be restricted to a limited zone in the vicinity of the interacting region. When the cutting laser beam is moving along the path of the preheating beam, with the distance between the two beams more than the keyhole depth, the cutting laser acts on a pool of cooling melt left by the first beam. Under such conditions, the cutting effect (depth, speed) will be dependent on the temperature distribution in the interaction zone caused by the preheating beam, as well as the characteristics of the cutting beam.

Material removal in laser cutting occurs by evaporation near the top surface and by ejection of slag and molten metal through the bottom surface. The sources for energy input are absorbed laser power, chemical power from the gas–metal reactions and mechanical power from the gas flow for ejecting the fluids. The energy dissipates by vaporization, melting, and ejection of the liquid, heat conduction into the sheet and convection cooling by the gas flow. In our analysis, we assume a moving line source thermal model to describe the temperature distribution in an isolated sheet of the molten region of the workpiece which surrounds the keyhole of the first moving laser beam. Carslaw and Jaeger [15], and Swifthook and Gick [16] provided the steady state solution for a moving line source as

$$T(x, y) = \frac{aP_1}{2\pi K Z_K} \exp(X) K_0(R) \qquad (11)$$

where T is the temperature (K), x the length dimension (m), y the width dimension (m), z the thickness dimension (m), a the absorption coefficient, P_1 the laser power of the first beam (W), K the thermal conductivity (W m^{-1} K^{-1}), Z_K the depth of keyhole (m), X a dimensionless variable, $xV/2\alpha$, V the cutting speed (m s^{-1}), α the thermal diffusivity (m^2 s^{-1}), and R a dimensionless variable $(x^2 + y^2)^{1/2} V/2\alpha$.

The line source model ignores the cut-width variation in the z-direction. The temperature distribution over the depth of workpiece near the keyhole was

calculated previously [17]. The expressions obtained connect keyhole and melt-pool depths with the characteristics of the laser beam. On the basis of these expressions and experimental results given by Kamalu and Steen [2], maximum keyhole depth may be estimated at a level of 6 mm and less, for our case, depending on the speed of the workpiece. Also, the isotherms obtained from Equation 11 may be considered to be a proper representation of the volumetric temperature distribution if the workpiece thickness, t, is near Z_K. At greater thicknesses the change from cylindrical geometry of heat-wave propagation to the spherical geometry near the tip of the keyhole becomes essential. Unfortunately, the above-mentioned model, regarding laser-beam penetration into a homogeneously preheated metal workpiece, cannot be used to find an exact solution to an inhomogeneous thermal distribution $T(x, y, z)$. However, estimates can be made by introducing an effective average temperature $\bar{T}(x, y) = (1/t)\int T(x, y, z)\,dz$. This average temperature is close to the value $\bar{T}(x, y)$ obtained by using Equation 15 with factor Z_K/t. Thus, the average temperature over the thickness of the workpiece, resulting from the action of the first laser beam, at the position of the second "cutting" laser beam is given by

$$\bar{T}(x, 0) = \frac{aP_1}{2\pi Kt}\exp(X)K_0(X) + T_a \qquad (12)$$

where T_a is the ambient temperature ($\simeq$ 300 K). In addition to the laser source, the chemical energy evolved from the oxidation of metal raises the average temperature. Hence Equation 12 is modified by incorporating the oxidation reaction as

$$\bar{T}(x, 0) = W + \frac{aP_1}{2\pi Kt}\exp(X)K_0(X) + T_a \qquad (13)$$

where $W = f_1 q/C$ (K), f_1 is the fraction of gas used for oxidation, q the heat of formation (J kg^{-1}), and C the specific heat (J kg^{-1} K^{-1}). The quantity W is difficult to estimate because of the complexity of oxidation phenomena, especially the unknown quantities including the composition of oxidation products, the proportion of the molten metal that is oxidized, and the latent heats of various phase transitions. The oxygen gas also contributes to the cooling of the melt. But the cooling effect has been shown to be negligible [2] if the gas flow is subsonic.

Assuming that the effective laser power absorption within the keyhole trap is approximately 0.8, and for a distance of 6 mm travelled by the first beam, the average temperature, $\bar{T}$, can be written as

$$\bar{T} = W + \frac{(0.8)P_1}{2\pi Kt}\exp\left(\frac{0.006V}{2\alpha}\right) \times K_0\left(\frac{0.006V}{2\alpha}\right) + T_a \qquad (14)$$

Equation 14 was solved and results are shown in Figs 6 and 7 for various degrees of preheating. Note that we have taken $W = 0$, because the gas jet nozzle diameter was so large that only a small fraction of oxygen was used for oxidation. Experimental data superimposed on these plots indicate that steel follows an isotherm of 500 K while superalloy preheats to an isotherm of 900 K. Equation 11 may also be used to estimate the kerf width if the second laser beam cuts through the thickness. Preheating of the metal by the first beam improves the absorption efficiency. Because the vicinity of the second beam–workpiece interaction is already in the melted condition, the absorption of the second beam is enhanced, and energy transfer through the keyhole becomes efficient, causing deep

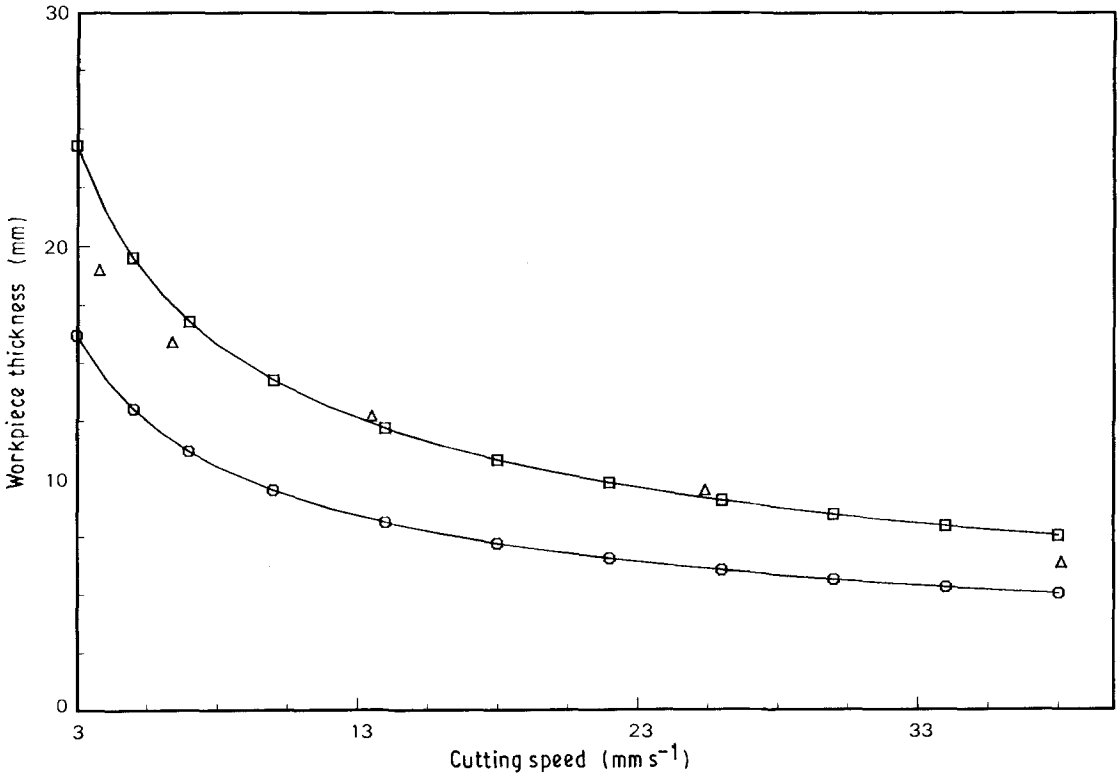

Figure 6 Workpiece thickness versus cutting speed for carbon steel at (□) 500 K, (○) 600 K; (△) experimental data.

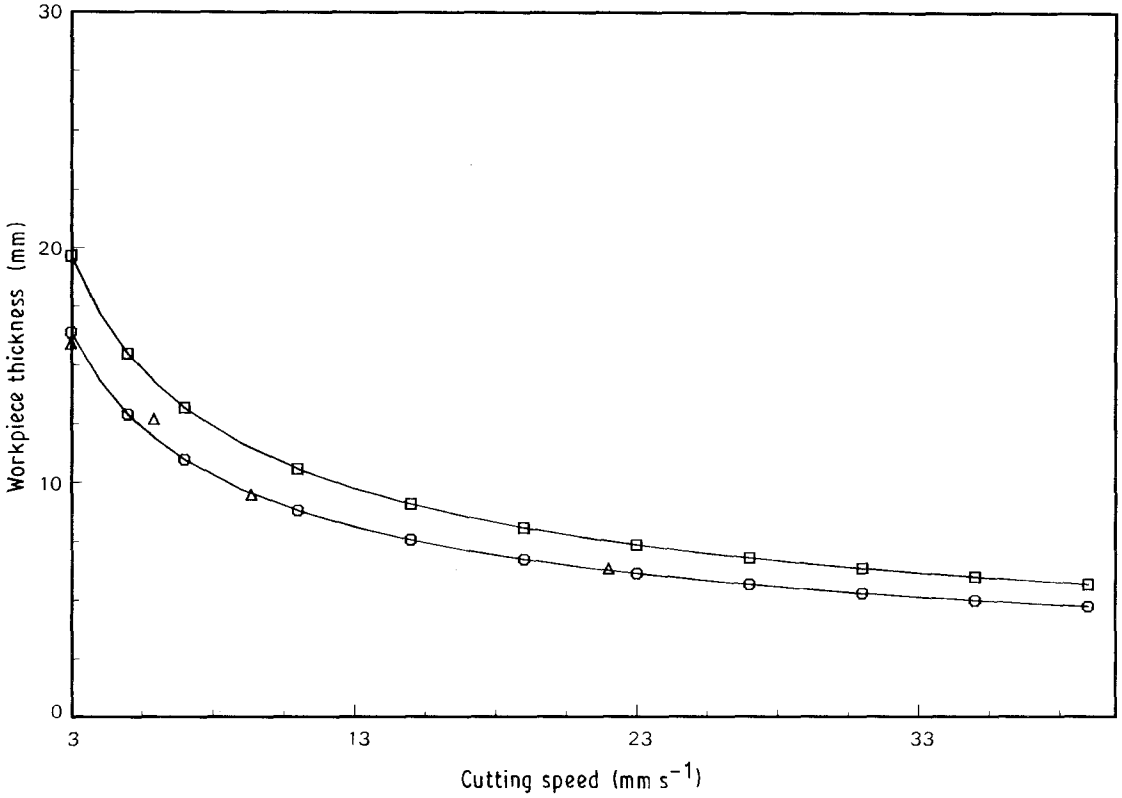

Figure 7 Workpiece thickness versus cutting speed for superalloy at (□) 800 K, (○) 900 K; (△) experimental data.

penetration. Swifthook and Gick [16] have given the following solutions to Equation 11 depending on the cutting speed.

Domain I For $Y_0 \leqslant 0.55$

$$Y_0 = \exp\left(1.5 - \frac{2\pi}{X_0}\right) \quad (15)$$

Domain II For $0.55 < Y_0 \leqslant 6.13$

$$Y_0 = f(X_0) \quad (16)$$

Domain III For $Y_0 > 6.13$

$$Y_0 = 0.483\, X_0 \quad (17)$$

where $X_0 = P_2/KT_m t$, $Y_0 = Vb/\alpha$, P_2 is the laser power of the second beam (W), and b the kerf width (m). Note that the exact function is not defined in Domain II. In fact, Domain II is of more practical interest. In this study, experimental data indicate that Y_0 is somewhere between 0.4 and 4.

Peretz and co-workers [18–20] have done extensive work on the effect of preheating on Swifthook and Gick's Equations 15, 16 and 17, and gave the following expression in Domain II

$$Y_0 = \frac{X_0 - 2}{1.9} \quad (18)$$

Babenko and Tychinskii [12] obtained a similar expression in gas-jet laser cutting as

$$Y_0 = \frac{X_0 - 1.885}{1.9} \quad (19)$$

If the workpiece is preheated, then

$$X_0 = \frac{P_2}{K(T_m - \bar{T})}\frac{1}{t} \quad (20)$$

Equation 18 has been modified by Peretz *et al.* [19] to include the effect of latent heat of fusion. For Domain II

$$X_0 = 2 + \left[1.9 + \frac{1.67L}{C(T_m - \bar{T})}\right] Y_0 \quad (21)$$

where L is the latent heat of fusion, 275×10^3 J kg^{-1} for steel, 300×10^3 J kg^{-1} for superalloy. Oxidation of metal and power for mechanically ejecting the slag/molten fluid should be included in the above equation as W_1. Equation 21 can be written as

$$X_0 = W_0 + \left[1.9 + \frac{1.67L}{C(T_m - \bar{T})}\right] Y_0 \quad (22)$$

where $W_0 = W_1 + 2$

Equation 22 can be simplified as

$$T_m - \bar{T} = \left(\frac{P_2}{Kt} - \frac{1.67L}{C}\frac{Vb}{\alpha}\right) \Big/ \left(W_0 + 1.9\frac{Vb}{\alpha}\right) \quad (23)$$

Fig. 8 was obtained from Equation 23 and shows the variation of Vb as a function of workpiece thickness, t. W_0 is the dimensionless empirical coefficient equal to 0.2 for carbon steel and 7 for superalloy. Equation 23 agrees well with experimental results and can therefore be used to predict the maximum cutting depth that can be obtained by an increase in the degree of preheating or by a decrease in the distance between the two laser beams. Fig. 9 shows the relationship between the maximum cut depth and the distance between the beams, d, at the minimum cutting speed, V_{min}. V_{min} was taken as 4.23 mm s^{-1} because at lower speeds there was considerable deterioration of the cut edges due to a "burn-out" effect.

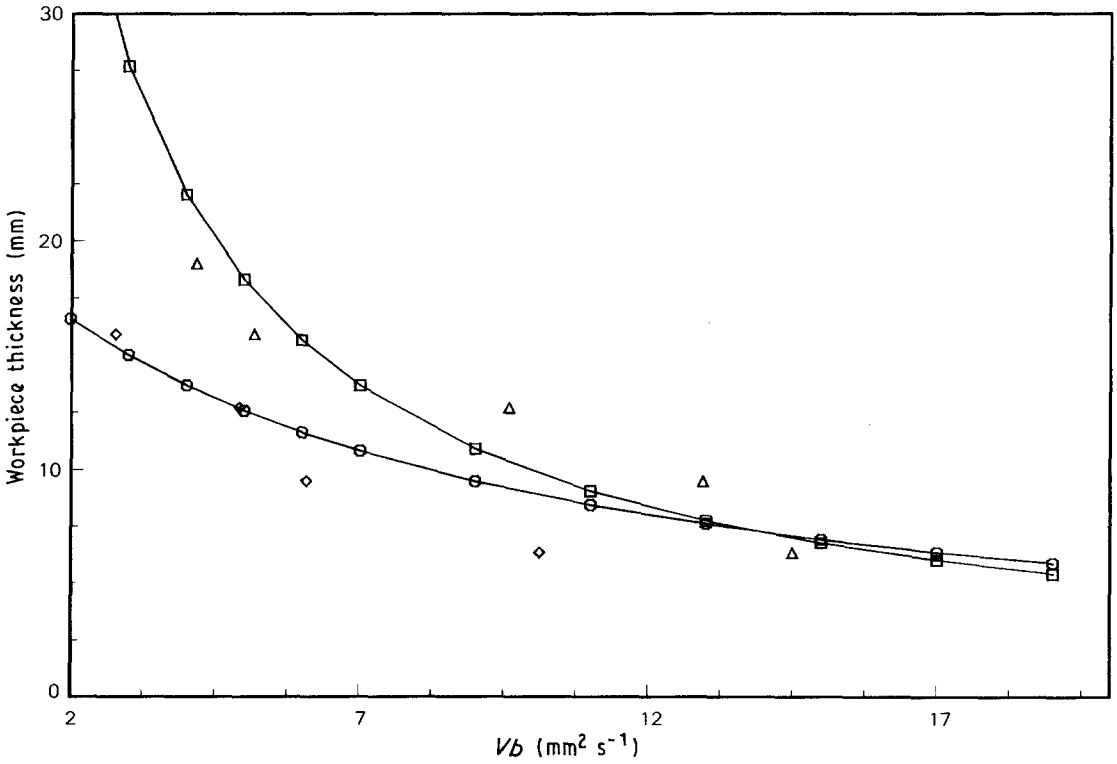

Figure 8 Workpiece thickness versus Vb for carbon steel and superalloy: (□) Carbon steel 500 K, (○) Superalloy 900 K; (△) Carbon steel experimental data, (◇) superalloy experimental data.

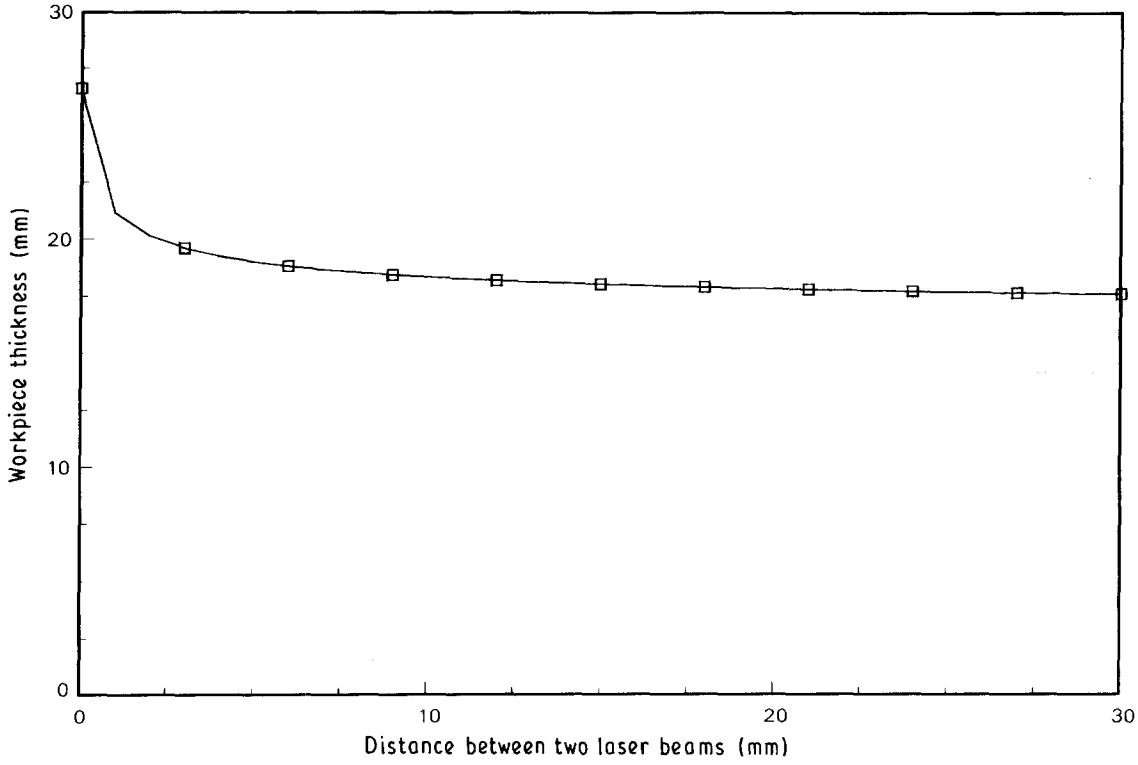

Figure 9 Workpiece thickness versus distance between two laser beams for carbon steel. $V = 4.23\ \text{mm s}^{-1}$.

From Fig. 9 it seems obvious that the best way to use two laser beams is to integrate them into one beam that has twice the power of either of the two individual beams. However, it should be noted that the model from which Fig. 9 was obtained was of linear source and may not be valid when the spacing between the two beams is less than the keyhole width.

One of the problems in the application of dual beam cutting is that due to the vibration of optical elements it is very difficult to achieve a stable coincidence with a precision better than the characteristic focal spot dimension (0.1 mm and less). In this case we obtain an irregular space distribution that can be likened to "dancing" TEM_{10} mode.

The effects of transfer from TEM_{00} and TEM_{10} mode on the cut quality were experimentally and theoretically investigated [21, 22]. On the basis of these results it may be concluded that for TEM_{10}

mode, a more stable cut quality may be achieved with the mode-poles oriented along the x-axis, that is, in the direction of the workpiece movement. This case may be considered as a stretching of the heat source in the direction of movement. By analogy, it looks promising, for the sake of cut quality, to introduce an initial shift, of about one keyhole width, between the two beams in the direction of movement. The result of this doubling or stretching of beam-width in the direction of movement, is an increase in γ, the angle between the cut front and the direction of the optical axis (see Fig. 10). For simplicity, the beam shapes are represented as cylinders. It is then quite obvious that γ depends upon the workpiece thickness, t, and the laser beam transverse dimension in the direction of movement, b_x ($\alpha = b_x/t$), and is about 2° at $t = 20$ mm for the usual one-beam case. From Petring *et al.* [23], it is evident that at this angle of cut-front inclination, Fresnel reflection causes a significant decrease in laser-beam absorption near the cut front. Also, maximum absorption is attained at angles that are approximately twice this angle. The results of the laser power absorption calculations for TEM_{03} mode [23] offer additional evidence to support the advantages of laser-spot stretching in the cutting direction.

Thus, an important practical conclusion that may be drawn, in the case of high-thickness cutting, is that stretching the width of the laser beam in the direction of cutting may favour increased power absorption and hence increased cut speed. In addition, it should be taken into account that the transverse dimension of the laser beam is comparable with the thickness of the melted layer on the cutting front. Pulsations of this layer due to the instability of the melt ejection process cause instabilities in the laser power input. The thickness of the molten-layer pulsation is proportional to the square root of the amplitude of the absorbed laser power oscillations and is directly connected with the width of the cut-edge striations [24]. It seems quite obvious that in the case of increasing γ, if the dimension of the laser beam is increasing in comparison with the molten layer thickness, there should be an improvement in laser-beam absorption stability and hence damping of the striations.

Fig. 11 represents the possible configurations of a two-beam optical system programmed for cutting when lasers with stable and unstable resonators are used. Mirror M_t may be electronically tilted synchronously with the CNC worktable so that the movable beam always precedes the cutting one in the direction of cutting.

From all that has been said, it would seem quite logical to modify the two-beam concept into an elliptical beam concept. Such beam configuration is especially promising in the case of cutting with high-power laser beams (> 5 kW) when the effect of plasma screening becomes essential. The elliptical focusing gives, in this case, the best compliance of a high-power laser beam with a narrow cut. It is known that the greatest cutting depth can be obtained when the focal point is submerged inside the workpiece. But it is usually complicated by a resulting higher cut width at the top edge of the cut slot and worse efficiency of laser-beam admittance into the cut. Fig. 12 illustrates an optical configuration for the elliptical beam cutting. The additional concave cylindrical lens, L_c, is fixed above the spherical focusing lens, L_s, with a focus length of about several metres determined by the

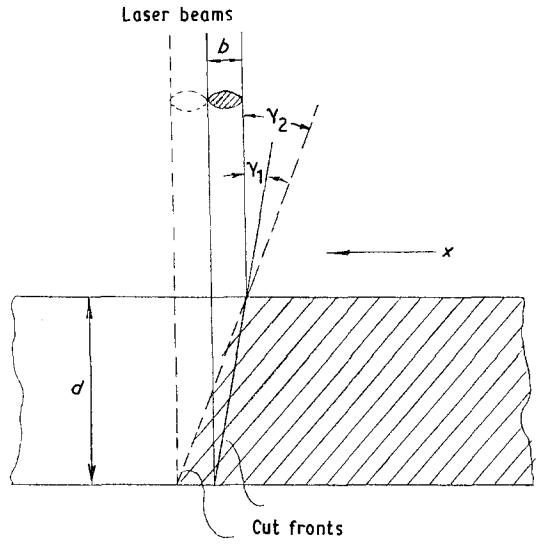

Figure 10 Schematic representation of the cut-front inclination increase with two adjacent laser beams.

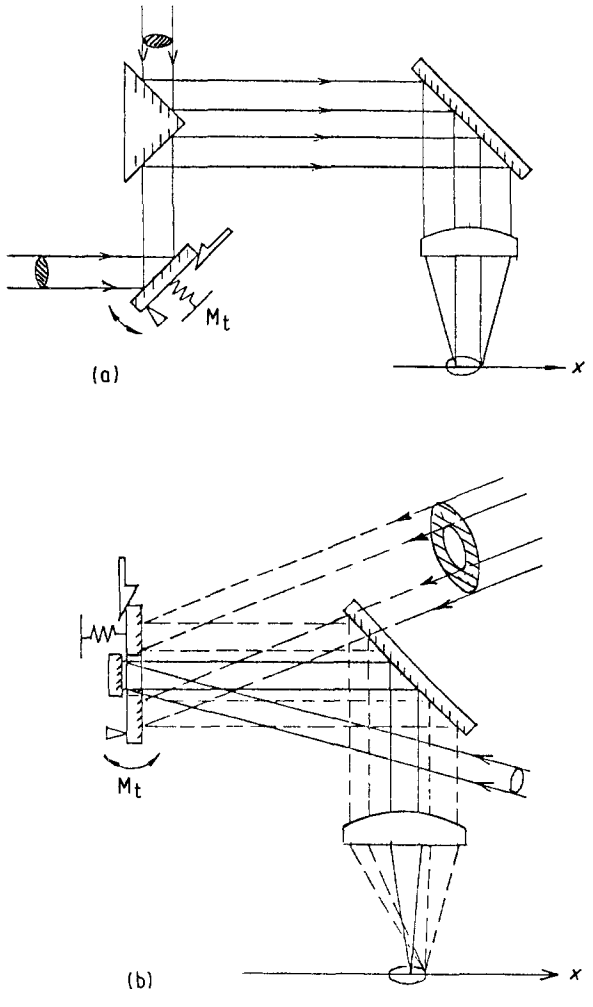

Figure 11 Optical arrangements for the integration of laser beams in a two-beam technique. (a) Two beams from stable laser cavities. (b) One of the beams emerges from an unstable laser cavity.

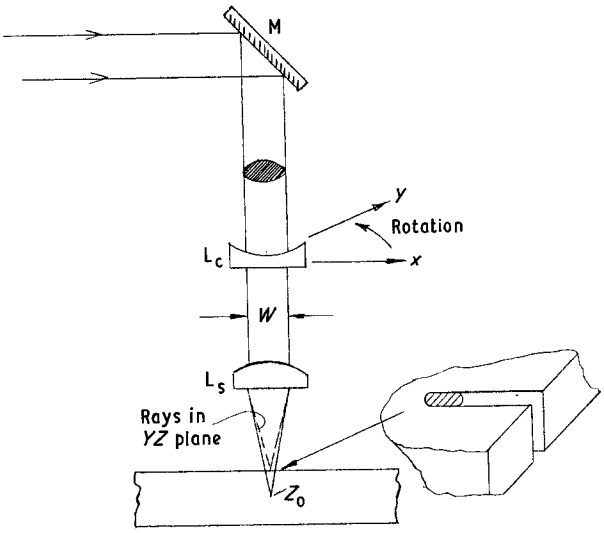

Figure 12 Proposed scheme for laser cutting with an elliptically focused beam.

relation

$$F = W/\omega\eta \tag{24}$$

where W is the diameter of the laser beam on a lens, ω the full angle divergency of the laser beam, and $\eta = l_x/l_y$. The cylindrical lens has a drive of angular rotation in the xy plane that can be synchronized with the CNC worktable for performing curved cuts.

In the present case, due to the guidance of radiation by the walls of the cut slot, maximum intensity is reached at the point Z_0 corresponding to a combined focus of the cylindrical and spherical lenses. However, at the same time the transverse dimension of the beam (the yz plane perpendicular to the cut direction) on the workpiece surface where the spherical lens is focused, is minimal.

6. Conclusions

Experimental and analytical studies of dual-beam CO_2 laser cutting of a carbon steel and a nickel-base superalloy yielded several interesting results.

1. Dual-beam CO_2 laser cutting can be performed at higher speeds than possible in single-beam CO_2 laser cutting.
2. The dual-beam method enhanced cutting thickness. This is especially useful for difficult to machine metals and alloys.
3. Heat-flow models were developed to predict the experimental results.
4. In the case of high-thickness cutting, stretching the width of the laser beam in the direction of cutting may favour increased power absorption and hence increased cut speed.

Acknowledgements

The author thanks Mr Srikanth and Beltran, Inc., for their assistance. This work was partially supported by the National Science Foundation under Grant Number ISI-8860788 and the Iowa Department of Economic Development.

References

1. The Editor, *Modern Machine Shop J.* September (1984) 21.
2. J. N. KAMALU and W. N. STEEN, "Laser Materials Processing", edited by M. Bass (North-Holland, Amsterdam, 1983) Ch. 2.
3. D. BELFORTE and M. LEVITT (eds). "Industrial Laser Annual Hand Book", SPIE Vol. 1241 (Pennwell, Tulsa, OK, 1990).
4. R. ROTHE and G. SEPOLD, "Important requirements on laser beam cutting systems for cutting thick plates", Laser Advanced Materials Processing (High Temperature Society of Japan, Osaka, 1987) pp. 251–3.
5. B. A. WARD, J. FIERET and M. J. TERRY, in SPIE Vol. 801, "High Power Lasers" (SPIE, 1987) pp. 243–50.
6. J. M. KAMALU, *Soc. Photo Instrum. Eng.* **621** (1986) 49.
7. P. A. MOLIAN, in "Proceedings of an International Conference on Laser Advanced Materials Processing", (High Temperature Society of Japan, Osaka, Japan, May 1987), pp. 251–3.
8. I. DECKER, J. RUE and W. ATZERT, *Proc. SPIE* September (1983) 81.
9. J. F. READY, "Effects of High Power Laser Radiation" (Academic Press, New York, 1971).
10. W. W. DULEY, "Laser Processing and Analysis of Materials" (Plenum, New York, 1983).
11. W. W. DULEY and J. N. GONSALVES, *Canad. J. Phys.* **50** (1972) 215.
12. V. P. BABENKO and B. TYCHINSKII, *Sov. J. Quantum Electron.* **2** (1973) 399.
13. K. A. BUNTING and G. CORNFIELD, *Trans. ASME J. Heat Transfer* February (1975) 116.
14. D. SCHUÖCKER and W. ABEL, *Proc. SPIE* September (1983) 88.
15. H. S. CARSLAW and J. C. JAEGER, "Conduction of Heat in Solids" (Clarendon Press, Oxford, 1962) pp. 255–72.
16. D. T. SWIFTHOOK and A. E. F. GICK, *Weld. Res. Suppl.* (1973) 492.
17. H. E. CLINE and T. R. ANTHONY, *J. Appl. Phys.* **48** (1977) 3895.
18. R. PERETZ, *Optics Lasers Engng* **9** (1988) 23.
19. *Idem, ibid.* **10** (1989) 3.
20. *Idem, ibid.* **7** (1987) 69.
21. P. Y. LUCIANI, C. CHANISSOUX and J. N. CALVET, in "Proceedings of the 3rd International Conference on Lasers in Manufacturing" (1986) pp. 117–22.
22. J. POWELL, K. FRASS and I. A. MENZIES, in "Proceedings of International Conference Laser 4: High Power Lasers in Metal Processing" (1988) pp. 310–26.
23. D. PETRING, P. ABELS and E. BEYER, in SPIE, Vol. 1020, "High Power CO_2 Laser Systems and Applications" (SPIE, 1988) pp. 123–31.
24. D. BECKER and W. SCHULTZ, in "Proceedings of the International Conference Laser/Optoelectronics in Engineering", Germany (1985) pp. 345–8.

Received 29 May
and accepted 2 November 1991